



Representing
time-dependent
freezing behaviour

R. J. Herbert et al.

This discussion paper is/has been under review for the journal Atmospheric Chemistry and Physics (ACP). Please refer to the corresponding final paper in ACP if available.

Representing time-dependent freezing behaviour in immersion mode ice nucleation

R. J. Herbert, B. J. Murray, T. F. Whale, S. J. Dobbie, and J. D. Atkinson

School of Earth and Environment, University of Leeds, Leeds, LS2 9JT, UK

Received: 29 November 2013 – Accepted: 28 December 2013 – Published: 17 January 2014

Correspondence to: R. J. Herbert (r.herbert@see.leeds.ac.uk) and B. J. Murray (b.j.murray@leeds.ac.uk)

Published by Copernicus Publications on behalf of the European Geosciences Union.

Title Page

Abstract

Introduction

Conclusions

References

Tables

Figures



Back

Close

Full Screen / Esc

Printer-friendly Version

Interactive Discussion



Abstract

In order to understand the impact of ice formation in clouds, a quantitative understanding of ice nucleation is required, along with an accurate and efficient representation for use in cloud resolving models. Ice nucleation by atmospherically relevant particle types is complicated by inter-particle variability in nucleating ability, as well as a stochastic, time-dependent, nature inherent to nucleation. Here we present a new and computationally efficient Framework for Reconciling Observable Stochastic Time-dependence (FROST) in immersion mode ice nucleation. This framework is underpinned by the finding that the temperature dependence of the nucleation rate coefficient controls the residence-time and cooling-rate dependence of freezing. It is shown that this framework can be used to reconcile experimental data obtained on different time scales with different experimental systems, and it also provides a simple way of representing the complexities of ice nucleation in cloud resolving models. The routine testing and reporting of time-dependent behaviour in future experimental studies is recommended, along with the practice of presenting normalised datasets following the methods outlined here.

1 Introduction

Clouds are known to exert a significant radiative impact on the Earth's energy budget with low clouds making the largest net contribution due to their dominating albedo effect and global spatial extent (Hartmann et al., 1992). Observational studies have shown that these clouds are commonly supercooled and can exist in a mixed-phase state (Zhang et al., 2010). Sassen and Khvorostyanov (2007) showed that the radiative properties of these mixed-phase clouds are dominated by the supercooled liquid phase, with increasing ice content decreasing their cooling effect. Therefore, along with cloud lifetime effects an enhanced ice formation process could lead to a significant climatic radiative impact. The formation and sublimation of ice particles also has

ACPD

14, 1399–1442, 2014

Representing time-dependent freezing behaviour

R. J. Herbert et al.

Title Page

Abstract

Introduction

Conclusions

References

Tables

Figures

◀

▶

◀

▶

Back

Close

Full Screen / Esc

Printer-friendly Version

Interactive Discussion



direct impacts on cloud dynamics through latent heat processes (Dobbie and Jonas, 2001), and the cold rain process, estimated to account for 50 % of all precipitation in mid-latitude regions and 30 % in tropical regions (Lau and Wu, 2003), is sensitive to the cloud ice water content. Therefore a thorough understanding of how ice is formed, along with an appropriate representation in models, is clearly important for correctly quantifying the impact of clouds on climate and weather.

In the atmosphere relatively pure liquid droplets will tend to supercool down to around 237 K before freezing homogeneously. The inclusion of an ice nucleating particle (IN) can act as a catalyst and allow freezing to occur at warmer temperatures. This process is generally split into four primary pathways determined by the interaction between the IN and the parent phase (Vali, 1985): immersion freezing occurs when the IN is immersed within a supercooled liquid droplet; contact freezing through the collision between an IN and the air–liquid interface of a supercooled droplet; deposition mode occurs under water subsaturated conditions via deposition of water vapour directly onto the IN surface; and condensation mode involves the condensation of water vapour onto the IN prior to freezing. Observational studies of mixed-phase clouds above homogeneous freezing temperatures show strong evidence that ice formation depends on the presence of supercooled liquid water droplets, (Abbatt and Nowak, 1997; Ansmann et al., 2009; de Boer et al., 2011; Field et al., 2012; Westbrook and Illingworth, 2013), which suggests that deposition and condensation mode ice nucleation below water saturation play a secondary role. Contact nucleation is not thought to be significant in deep convection (Cui et al., 2006; Phillips et al., 2008), but may be important in some situations, particularly where droplets are evaporating (Ansmann et al., 2005; Ladino et al., 2013). This study focuses on the immersion freezing mode due to its potential primary atmospheric importance.

Heterogeneous ice nucleation is fundamentally a stochastic process, meaning that the probability of nucleation depends on both the IN surface area and the time available for nucleation. In addition to the variability of freezing temperature associated with the stochastic nature of nucleation, there is often a strong inter-particle variability with

Representing time-dependent freezing behaviour

R. J. Herbert et al.

Title Page

Abstract

Introduction

Conclusions

References

Tables

Figures



Back

Close

Full Screen / Esc

Printer-friendly Version

Interactive Discussion



some particles capable of nucleating ice at much higher temperatures than others. The ability for an IN to catalyse ice nucleation is dependent on its physiochemical properties; these may be crystallographic, chemical, or surface features such as cracks or defects that provide sites where the energy barrier to nucleation is at a local minimum (Pruppacher and Klett, 1997).

Experimental studies have shown that atmospherically relevant IN exhibit an extremely diverse range in their ability to nucleate ice heterogeneously (Murray et al., 2012; Hoose and Möhler, 2012). Along with this variability in nucleating ability, the importance of the stochastic, time-dependent, nature of ice nucleation is also reported to vary between IN species. Repeated freezing cycles of single droplets performed by Vali (2008) with two soil samples resulted in < 1 K variation in freezing temperatures, which was much smaller than the variability in freezing temperature over an array of droplets. On this basis Vali (2008) argued that the time-dependence of nucleation is of secondary importance. Similarly Ervens and Feingold (2013) recently performed a sensitivity study which highlighted changes in temperature as being the most important factor in droplet freezing sensitivity. In contrast, other studies have concluded that the time-dependence of nucleation is important. For example, Kulkarni and Dobbie (2010) used a deposition mode stage and reported that the fraction of dust particles activated to ice increased with time under constant temperature and RH conditions. Using an immersion mode cold-stage instrument with cooling rates from 1 to 10 K min^{-1} , Murray et al. (2011) found that the freezing of droplets containing kaolinite (KGa-1b) was consistent with a stochastic model which required no inter-particle variability. Broadley et al. (2012) used the same instrument with the mineral dust NX Illite and found that under isothermal conditions nucleation continued with time. Similarly, Welti et al. (2012), using an ice nucleation chamber to test their kaolinite sample (K-SA), found that the fraction of droplets frozen increased with increasing residence time. Wilson and Haymet (2012) have shown that repeated freezing and thawing cycles for a single droplet results in a distribution of freezing temperatures. The width of this distribution varies for different droplets and different materials, potentially indi-

Representing time-dependent freezing behaviour

R. J. Herbert et al.

Title Page

Abstract

Introduction

Conclusions

References

Tables

Figures

◀

▶

◀

▶

Back

Close

Full Screen / Esc

Printer-friendly Version

Interactive Discussion



Representing time-dependent freezing behaviour

R. J. Herbert et al.

Title Page

Abstract

Introduction

Conclusions

References

Tables

Figures



Back

Close

Full Screen / Esc

Printer-friendly Version

Interactive Discussion



cating a range of time-dependent behaviour. More recently, Wright and Petters (2013) performed a series of freeze-thaw simulations and found that the mean variation in freezing temperature for their ensemble of droplets was dependent on the slope of the nucleation rate coefficient $d\ln(J)/dT$, with cooling rate and IN surface area having little effect on the observed variation. In summary, the stochastic nature of nucleation in some materials is more important or more apparent than in others. In order to fully understand the impact of different IN species and populations on clouds it is important to both fundamentally understand the nucleation mechanism and correctly represent this process in an efficient framework for use in cloud resolving models (CRMs).

The main objective of the work presented in this paper is to develop a framework that can be used to describe the time-dependence of nucleation as well as the inter-particle variability inherent to many nucleating materials. In this study we use a multiple component stochastic model to establish the key relationships between the physical properties of an IN and its observable time-dependent behaviour, which are then captured in a simple framework. This framework bears some resemblance to the empirically derived modified singular description presented by Vali (1994), but here we link the term describing the residence-time and cooling-rate dependence to the temperature dependence of the nucleation rate coefficient. We then go on to use this framework to analyse several experimental datasets and discuss the implications for modelling ice nucleation in cloud models.

1.1 Immersion mode freezing models

1.1.1 The single-component stochastic freezing model

Nucleation is thought to be a process where random fluctuations in ice-like clusters within a supercooled droplet result in a freezing event only if a cluster reaches a critical size. For homogeneous nucleation, the probability of a critical cluster forming is increased for both larger droplet volumes and longer time scales. The inclusion of particles which can serve as an IN provides a surface which favours cluster formation

and therefore catalyses nucleation. The probability of a droplet freezing in this mode is a stochastic, time-dependent process with the temperature-dependent nucleation rate coefficient $J(T)$ expressed per unit surface area, per unit of time. In the single-component stochastic freezing model it is assumed that every IN within a population can be described with the same $J(T)$, which is consistent with nucleation by some materials (Murray et al., 2011). Classical nucleation theory (CNT) can be used to link $J(T)$ to a conceptual contact angle, θ , which is defined as the angle between the particle and ice cluster and is used as a measure of how efficiently a material nucleates ice.

1.1.2 Singular freezing models

Singular or deterministic models have been developed in light of the observation that the variability in freezing temperatures for an entire population of droplets in a cooling experiment can be significantly higher than that of a single droplet upon multiple refreezing cycles (e.g. Vali, 2008). The range of freezing temperatures can also be much greater than the shift in temperature observed for a change of cooling rate. These observations have been used to argue that the time-dependence of nucleation is of secondary importance in comparison to the inter-particle variability in atmospheric aerosol (Vali, 2008). The reason why there is such strong inter-particle variability in ice nucleating ability is very poorly understood, but could arise for a number of reasons: inhomogeneity of surface properties such as cracks, grain boundaries or pores have been shown to preferentially trigger nucleation (Pruppacher and Klett, 1997); a complex ice nucleating population with multiple constituent IN species, such as may exist within soil, could also present a range of nucleating efficiency within a single population (Conen et al., 2011; Atkinson et al., 2013); and small inclusions of a very active material, such as lead containing nanoparticles, can dominate and thus determine the ice nucleating ability of larger “host” particles (Cziczo et al., 2009). The concept of active sites has been introduced to describe this heterogeneity in ice nucleating ability in many samples, and singular freezing models have been developed to link this variable distribution to the freezing probability (Levine, 1950; Vali, 1971; Connolly et al., 2009;

Title Page

Abstract

Introduction

Conclusions

References

Tables

Figures

◀

▶

◀

▶

Back

Close

Full Screen / Esc

Printer-friendly Version

Interactive Discussion



Sear, 2013). Nucleation on active sites, whatever their physical form, is a stochastic process (as will be discussed in Sect. 1.13 below), but within the singular model it is assumed that a particle or active site on that particle will trigger ice nucleation at a specific temperature independent of time. An advantage of this simplifying assumption is that the varying ice nucleating efficiency of a population or species can be represented as a simple function of temperature.

1.1.3 Multiple-component models

In order to satisfy both the stochastic nature of ice nucleation and the varying efficiency of IN in a physically based framework, a number of multiple-component models have been developed. These descriptions use a distribution of sites or droplets displaying a range of nucleating characteristics to describe the ice nucleating variability. Each component is assumed to approximate to a single-component model with a single function describing the nucleation rate against temperature.

Marcilli et al. (2007) used a variety of probability density functions (PDFs) to represent populations of particles, each characterised by a particular contact angle ($0 \leq \theta \leq \pi$), in order to fit CNT to their immersion freezing data. This was then extended to include an active site distribution, which assumed that a single IN may have multiple nucleation sites on its surface, determined by the probability of an active site occurring per contact angle. A proportion of nucleating surface area per contact angle was then calculated assuming a standard size for a single active site; thus, larger particles will be more likely to contain sites of better nucleating ability than smaller particles. Lüönd et al. (2010) used a similar method to reconcile their experimental data. A multiple-component framework capable of describing both internally and externally mixed populations was presented by Murray et al. (2011). This was extended by Broadley et al. (2012) into the Multiple Component Stochastic Model (MCSM), which replaced CNT with a simple function to describe $J(T)$ for each component. In their study this function was systematically adjusted using a Gaussian distribution to represent a population with varying droplet freezing ability and is discussed in more detail

Representing time-dependent freezing behaviour

R. J. Herbert et al.

Title Page

Abstract

Introduction

Conclusions

References

Tables

Figures

◀

▶

◀

▶

Back

Close

Full Screen / Esc

Printer-friendly Version

Interactive Discussion



Representing time-dependent freezing behaviour

R. J. Herbert et al.

Title Page

Abstract

Introduction

Conclusions

References

Tables

Figures

◀

▶

◀

▶

Back

Close

Full Screen / Esc

Printer-friendly Version

Interactive Discussion



in Sect. 2. The “Soccer ball model” was developed by Niedermeier et al. (2011) using a similar approach to Marcolli et al. (2007): in their description each particle is divided into a number of sites or patches, with each site randomly assigned a contact angle ($0 \leq \theta \leq \pi$) from a Gaussian distribution. It can be seen that having a small number of sites per IN will result in a population with diverse ice nucleating ability, whereas more sites will increase the probability of a specific site occurring per IN, so that the population tends towards a uniform nucleating ability.

All of these multiple-component models can be used to describe the inter-particle variability of ice nucleating efficiency within a population, and also the fundamental stochastic nature of ice nucleation. However, a significant increase in complexity is introduced through the treatment of separate populations and PDFs. Due to this, their use in CRMs is limited. Clearly, a framework is required that can adequately describe variable ice nucleating ability and stochastic behaviour in a computationally efficient way.

2 The Multiple Component Stochastic Model

The MCSM divides a population of particles, or nucleation sites, into sub-populations of equally efficient entities. Each sub-population can then be treated as a single component with a uniform nucleating behaviour allowing the use of the single-component stochastic freezing model; the summation of these populations then represents the entire population. Assuming each droplet contains a single IN with surface area s (cm^2) we can calculate the number of droplets that will freeze in a time increment δt at temperature T for a single component, denoted by i :

$$n_{\text{frozen},i} = n_{\text{liquid},i} (1 - \exp(-J_i(T) \cdot s_i \cdot \delta t)), \quad (1)$$

where $n_{\text{liquid},i}$ is the number of liquid droplets at the beginning of the time step, $n_{\text{frozen},i}$ is the number of frozen droplets, and $J_i(T)$ is the nucleation rate coefficient ($\text{cm}^{-2} \text{s}^{-1}$).

The exponential term describes the fractional probability P_{NOT} of an event not happening, where $P_{\text{NOT}} \rightarrow 1$ represents an increasing probability for no event to occur. For this study we use a simple linear temperature-dependent function to define $J_i(T)$ of a single component following Broadley et al. (2012) and Wright and Petters (2013):

$$\ln(J_i(T)) = \lambda_i T + \varphi_i, \quad (2)$$

where λ_i represents the gradient of $\ln(J_i(T))$ and φ_i the relative nucleating efficiency of the component. Others have used CNT to describe the temperature dependence of J (Marcolli et al., 2007; Lüönd et al., 2010; Niedermeier et al., 2011), but measured nucleation coefficients approximate to Eq. (2) over the range of freezing temperatures observed during a single freezing experiment (typically < 10 K) (Kashchiev et al., 2009; Stan et al., 2009; Ladino et al., 2011; Murray et al., 2010, 2011).

In order to extend Eq. (2) to multiple-component systems, each sub-population, behaving as an independent single component, is characterised by a specific φ_i and then weighted using a Gaussian function to calculate a probability of occurrence $P(\varphi_i)$, with mean μ and standard deviation σ (see Fig. 1). Thus, the number of droplets in each sub-population is $n_{\text{liquid},i} = N \cdot P(\varphi_i)$ where N is the total number of droplets in the experiment. The MCSM can now be defined by summing the number of droplets frozen in each sub-population for a given time increment:

$$N_{\text{frozen}} = \sum_{i=1}^n n_{\text{liquid},i} (1 - \exp(-J_i(T) \cdot s_i \cdot \delta t)). \quad (3)$$

To investigate the sensitivity of the MCSM to time-dependence (manifesting as a cooling-rate and residence-time dependence) an idealised box model was used to represent an immersion mode droplet freezing experiment under constant cooling or isothermal conditions in which droplet volume was assumed to be constant with no condensational growth or evaporation. Freezing events were assumed to only occur within a single time step and within the bulk volume. Additionally, freezing of one droplet was assumed to have no effect on the remaining liquid population.

Representing
time-dependent
freezing behaviour

R. J. Herbert et al.

Title Page

Abstract

Introduction

Conclusions

References

Tables

Figures



Back

Close

Full Screen / Esc

Printer-friendly Version

Interactive Discussion



3 Deriving a new immersion mode framework

3.1 Cooling-rate dependence

In these simulations we look at the sensitivity of the MCSM to changes in cooling rate. The aim is to identify the variables that control the cooling-rate dependent behaviour of a population of droplets. On inspection of Eq. (3) it is evident that for a constant finite increment δT , an increase in cooling rate results in a similar decrease in time δt , and therefore a decrease in the probability of a freezing event occurring between T and $T + \delta T$. This is manifested in the number of droplets freezing per δT and results in the entire cumulative fraction frozen curve shifting to lower temperatures. This is demonstrated in Fig. 2, with two simulated populations of droplets: one with a uniform IN distribution (a single value of φ_i) and the other with a diverse IN distribution (broad range of φ_i). Both populations have $\lambda = -2$ where λ is defined as $d \ln(J_i) / dT$ (i.e. the temperature dependence of the nucleation rate coefficient for each component). The droplets were cooled at 1 and 10 Kmin^{-1} . Figure 2 illustrates how the shift in temperature (β) for a change in cooling rate is independent of the distribution of φ_i . The independence of β to the distribution of φ_i has been further investigated using a series of droplet cooling simulations where all the free variables in the MCSM were allowed to vary between runs, with the corresponding values shown in Table 1. The results from these simulations, shown in Fig. 3, show that the only characteristic of the IN population required to quantify its cooling-rate dependence is λ ($d \ln(J_i) / dT$). This is a similar conclusion to Broadley et al. (2012) and Wright and Petters (2013).

This result can be understood by rearranging Eq. (1) to describe the change in temperature required to attain a specific cumulative frozen fraction for a given change in cooling rate (see the Supplement for the full derivation). For a given population of droplets containing an immersed IN, the total fraction of droplets frozen $f(n_i) =$

ACPD

14, 1399–1442, 2014

Representing time-dependent freezing behaviour

R. J. Herbert et al.

Title Page

Abstract

Introduction

Conclusions

References

Tables

Figures



Back

Close

Full Screen / Esc

Printer-friendly Version

Interactive Discussion



$n_{\text{liquid}}/n_{\text{frozen}}$ upon cooling from T_0 to T_{n_r} in n_r steps can be described by:

$$f(n_r) = 1 - \prod_{k=0}^{n_r} (\exp(-J(T_k) \cdot s \cdot \delta t)) = 1 - \exp\left(-\sum_{k=0}^{n_r} J(T_k) \cdot s \cdot \delta t\right), \quad (4)$$

where n_r denotes the total number of model steps using a cooling rate r , and δt is the time between steps k and $k+1$. As in Eq. (1) the exponential term essentially describes the cumulative probability of a freezing event not occurring in n_r time steps, and can be expanded so that $J(T_k) = J(T_0) \cdot (\exp(\lambda \delta T))^k$. By substituting Eq. (2) into Eq. (4) we can explicitly represent the nucleation rate coefficient:

$$f(n_r) = 1 - \exp\left(-s \cdot \delta t \cdot J(T_0) \sum_{k=0}^{n_r} (\exp(\lambda \delta T))^k\right). \quad (5)$$

The summation term can be removed using a geometric summation of series formula. Once rearranged we have a formula to calculate the temperature $T_{f(n)}$ at which a specific fraction frozen is reached:

$$T_{f(n)} = n_r \delta T = \ln \left[1 - \left(\frac{-\ln(1 - f(n_r)) \cdot (1 - \exp(\lambda \delta T))}{s \cdot \delta t \cdot J(T_0)} \right) \right] \frac{1}{\lambda} - 1, \quad (6)$$

where δT is the change in temperature between steps k and $k+1$. A change in cooling rate from r_1 to r_2 results in a change in the number of steps Δn_r to reach fraction f where $f = f_{n,r_1} = f_{n,r_2}$ and therefore a change ΔT_f :

$$\Delta T_f = n_{r_2} \delta T - n_{r_1} \delta T = \ln \left(\frac{C \cdot s \cdot \delta t_{r_2} \cdot J(T_0)}{C \cdot s \cdot \delta t_{r_1} \cdot J(T_0)} \right) \cdot \frac{1}{\lambda}, \quad (7)$$

where δT is constant for both cases, δt is dependent on the cooling rate, and $C = -\ln(1 - f) \cdot (1 - \exp(\lambda \delta T))$. Cancelling terms in Eq. (7) and substituting $r_1 = \delta T / \delta t_{r_1}$

Representing time-dependent freezing behaviour

R. J. Herbert et al.

Title Page

Abstract

Introduction

Conclusions

References

Tables

Figures

◀

▶

◀

▶

Back

Close

Full Screen / Esc

Printer-friendly Version

Interactive Discussion



and $r_2 = \delta T / \delta t_{r_2}$ provides a formula for the change in temperature, β_{cool} , observed at a specific fraction frozen for a given change in cooling rate:

$$\Delta T_f = \beta_{\text{cool}} = \frac{1}{-\lambda} \ln \left(\frac{r_1}{r_2} \right). \quad (8)$$

Equation (8) is consistent with the results shown in Fig. 2, i.e. the systematic shift in cumulative fraction frozen for a change in cooling rate is only dependent on λ . Vali (1994) empirically found a similar relationship where $\beta_{\text{cool}} = 0.66 \cdot \ln(r_1/r_2)$. In our independently derived expression, we take the additional step of linking β to λ , which offers a physical insight to the properties of a particular ice nucleating material, i.e. the empirical factor from Vali (1994) above relates to the gradient of the species $d\ln(J_i)/dT$. so that $0.66 = -\lambda^{-1}$ ($\lambda = -1.52$).

3.2 Residence-time dependence

In addition to droplet freezing experiments where droplets are cooled at some rate, other experiments (e.g. those using continuous flow diffusion chambers) involve exposing particles to a constant temperature for a defined period of time. In this section we show how measurements made with different residence-times under isothermal conditions in such instruments can be reconciled by extending the λ based formula presented in the previous section. Using $r = \Delta T/t$ the relative change in cooling rate described by $\ln(r_1/r_2)$ can also be expressed as a relative change in time $\ln(t_2/t_1)$:

$$\beta_{\text{iso}} = \frac{1}{-\lambda} \ln \left(\frac{t_2}{t_1} \right), \quad (9)$$

where β_{iso} is the shift in temperature required to produce the same frozen fraction in two isothermal experiments with duration times of t_1 and t_2 .

Representing time-dependent freezing behaviour

R. J. Herbert et al.

Title Page

Abstract

Introduction

Conclusions

References

Tables

Figures

◀

▶

◀

▶

Back

Close

Full Screen / Esc

Printer-friendly Version

Interactive Discussion



3.3 Reconciling droplet freezing data from different instruments and on different time scales

Since nucleation is a stochastic process, differences in experimental time scale and experimental technique need to be reconciled. First we reconcile isothermal data with cooling experiments so they are consistent with each other. This can be achieved by equating the simulated fraction frozen using both methods at the same temperature:

$$f_{\text{iso}}(T) = f_{\text{cool}}(T), \quad (10)$$

where “cool” denotes a cooling experiment simulation from $T_0 = 273.15$ K and “iso” an isothermal experiment simulation at a temperature T . The fraction frozen during an isothermal simulation is calculated similarly to a cooling experiment except the temperature remains constant throughout, thus we can use Eq. (4) to describe an isothermal simulation:

$$f_{\text{iso}}(T) = 1 - \prod_{k=0}^{n_{\text{iso}}} \exp(-J(T_k) \cdot s \cdot \delta t_{\text{iso}}), \quad (11)$$

$$J(T_k) = J(T), \quad (12)$$

therefore

$$f_{\text{iso}}(T) = 1 - \exp(-J(T) \cdot s \cdot \delta t_{\text{iso}} \cdot n_{\text{iso}}), \quad (13)$$

where n_{iso} is the total number of time steps, δt_{iso} , for the isothermal simulation. Substituting Eqs. (13) and (4) into Eq. (10) gives:

$$1 - \exp(-J(T_{n_{\text{cool}}}) \cdot s \cdot \delta t_{\text{iso}} \cdot n_{\text{iso}}) = 1 - \exp\left(-\sum_{k=0}^{n_{\text{cool}}} J(T_k) \cdot s \cdot \delta t_{\text{cool}}\right), \quad (14)$$

Title Page

Abstract

Introduction

Conclusions

References

Tables

Figures

◀

▶

◀

▶

Back

Close

Full Screen / Esc

Printer-friendly Version

Interactive Discussion



which, when simplified gives the total time (t_{total}) required for an isothermal experiment to reach the same fraction as a cooling experiment at temperature T :

$$\delta t_{\text{iso}} \cdot n_{\text{iso}} = t_{\text{total, iso}}(T_{n_{\text{cool}}}) = \frac{1}{J(T_{n_{\text{cool}}})} \sum_{k=0}^{n_{\text{cool}}} J(T_k) \delta t_{\text{cool}}. \quad (15)$$

5 Substituting in Eq. (2), after expanding as in Sect. 3.1, and rearranging gives:

$$t_{\text{total, iso}}(T_{n_{\text{cool}}}) = \delta t_{\text{cool}} \sum_{k=0}^{n_{\text{cool}}} (\exp(\lambda \delta T))^k. \quad (16)$$

Using a summation of series the summation term is removed and the formula can be simplified:

$$10 \quad t_{\text{total, iso}}(T_{n_{\text{cool}}}) = \frac{\delta t_{\text{cool}}}{1 - \exp(-\lambda \cdot \delta T_{\text{cool}})}. \quad (17)$$

A Taylor expansion of $\exp(-\lambda \cdot \delta T_{\text{cool}})$ will result in the series $\left[1 - \lambda \delta T_{\text{cool}} + 1/2(\lambda \delta T_{\text{cool}})^2 - 1/6(\lambda \delta T_{\text{cool}})^3 \dots\right]$. When $\lambda \delta T_{\text{cool}} \gg 1/2(\lambda \delta T_{\text{cool}})^2$, $\exp(-\lambda \delta T_{\text{cool}}) \cong 1 - \lambda \delta T_{\text{cool}}$. This is satisfied when the simulation temperature step $\lambda \delta T_{\text{cool}} \ll 1$. We can then simplify this formula using $r_{\text{cool}} = \delta T_{\text{cool}} / \delta t_{\text{cool}}$, where $r_{\text{cool}} < 0 \text{ K min}^{-1}$, so that:

$$15 \quad t_{\text{total, iso}}(T_{n_{\text{cool}}}) = \frac{\delta t_{\text{cool}}}{\lambda \cdot r_{\text{cool}} \cdot \delta t_{\text{cool}}} = \frac{1}{\lambda \cdot r_{\text{cool}}}. \quad (18)$$

20 Assuming that the nucleation rate coefficient of a species is approximated by the functional form in Eq. (2), this gives the time required for an isothermal experiment to reach the same frozen fraction as in a cooling rate experiment at a specific temperature. Again λ (the gradient of the nucleation rate coefficient) controls the time-dependent nature of immersion mode droplet freezing.

Representing time-dependent freezing behaviour

R. J. Herbert et al.

Title Page

Abstract

Introduction

Conclusions

References

Tables

Figures

◀

▶

◀

▶

Back

Close

Full Screen / Esc

Printer-friendly Version

Interactive Discussion



Now that isothermal and cooling experiments are reconcilable, results influenced by the cooling-rate and residence-time dependent behaviour of an IN in an experiment can be normalised to a standard rate r_{standard} , for which we have chosen -1 Kmin^{-1} . For cooling experiments, replacing r_1 in Eq. (8) with r_{standard} and r_2 with the experimental cooling rate r , in Kmin^{-1} , gives β as a function of the absolute cooling rate:

$$\beta(r) = \Delta T = \frac{1}{-\lambda} \ln \left(\frac{1}{|r|} \right). \quad (19)$$

For isothermal experiments, replacing r_{cool} with r_{standard} in Eq. (18) gives the time required for an isothermal experiment to be comparable to a normalised cooling experiment. Substituting t_1 in Eq. (9) with t_{total} in Eq. (18), and t_2 with the experimental residence time t , in seconds, gives β as a function of residence time:

$$\beta(t) = \Delta T = \frac{1}{-\lambda} \ln \left(\frac{-\lambda \cdot t}{60} \right). \quad (20)$$

Experimental data can then be modified and normalised using $T' = T_{\text{experiment}} - \beta$, where T' is the normalised temperature, and $T_{\text{experiment}}$ the temperature of the experiment data point.

For an IN species characterised by a specific λ , this immersion mode framework, named the Framework for Reconciling Observable Stochastic Time-dependence (FROST), can be used to reconcile and normalise data obtained through cooling and isothermal experiments.

3.4 Incorporating the FROST framework into a singular model

As discussed in Sect. 1.1.2, the singular model of ice nucleation is well suited to describing the inter-particle variability of ice nucleating ability, but it does not describe the time-dependent nature of nucleation. Nucleation probability is often described by the nucleation coefficient, $n_s(T)$, (sometimes called the active site density (DeMott, 1995)

or ice active surface site density, Connolly et al., 2009; Murray et al., 2012; Hoose and Möhler, 2012) which describes the cumulative number of freezing events that can occur between T_0 and T :

$$f(T) = 1 - \exp(-n_s(T) \cdot s). \quad (21)$$

Vali refers to a similar quantity (expressed per volume rather than surface area) as the cumulative nucleus spectrum (Vali et al., 1966; Vali, 1971). By rearranging Eq. (21) it can be seen that $n_s(T)$ (in units cm^{-2}) is directly related to the cumulative fraction frozen:

$$n_s(T) = -\frac{\ln(1 - f(T))}{s}. \quad (22)$$

It is therefore apparent that a systematic shift in the cumulative fraction frozen, caused by a change in the cooling rate or residence time, results in a systematic shift in $n_s(T)$ so that, upon incorporating Eq. (19) into Eq. (23) we find that for a specific cooling rate r :

$$f(T, r) = 1 - \exp\left(-n_s\left(T - \frac{\ln(|r|)}{\lambda}\right) \cdot s\right). \quad (23)$$

The differentiation of n_s with respect to T results in the function $k(T)$ that can be used to calculate the change in the fraction frozen occurring upon a change in T :

$$\Delta f(T, r) = 1 - \exp\left(-k\left(T - \frac{\ln(|r|)}{\lambda}\right) \cdot s \cdot \Delta T\right), \quad (24)$$

where $k(T)$ is the normalised nucleation coefficient in units $\text{cm}^{-2}\text{K}^{-1}$. Equation (24) is consistent with the empirical “modified singular” equation presented by Vali (1994), but here we have linked the stochastic term to the temperature dependence of the nucleation rate coefficient.

Representing
time-dependent
freezing behaviour

R. J. Herbert et al.

Title Page

Abstract

Introduction

Conclusions

References

Tables

Figures

◀

▶

◀

▶

Back

Close

Full Screen / Esc

Printer-friendly Version

Interactive Discussion



Similar equations can also be defined for isothermal experiments by incorporating Eq. (20) into Eq. (21) so that at a specific temperature, T_{iso} and residence time, t :

$$f(T, t) = 1 - \exp\left(-n_s \left(T - \frac{1}{-\lambda} \ln\left(\frac{-\lambda \cdot t}{60}\right)\right) \cdot s\right). \quad (25)$$

5 Again, upon differentiation we obtain an equation for the change in fraction frozen upon a change in residence time from t to $t + \Delta t$:

$$\Delta f(T, t) = 1 - \exp\left(-k \left(T - \frac{1}{-\lambda} \ln\left(\frac{-\lambda \cdot t}{60}\right)\right) \cdot s \cdot \frac{1}{\lambda \cdot t} \Delta t\right), \quad (26)$$

10 where $\Delta t/(\lambda \cdot t)$ has replaced ΔT through the incorporation of Eq. (18) into $\Delta T = r/60 \cdot \Delta t$; r is in Kmin^{-1} and Δt in seconds.

4 Testing the FROST framework

In the previous section we presented the FROST framework which is a new immersion mode ice nucleation framework designed to represent both the inter-particle variability of ice nucleating efficiencies and the stochastic (time-dependent) nature of nucleation.

15 In this section the FROST framework will be tested using a combination of original experimental droplet freezing data and literature data for atmospherically relevant IN obtained from a range of methods and instruments.

4.1 Kaolinite data (KGa-1b) from two cold-stage instruments

20 In this example data from droplet freezing experiments on two cold-stage instruments, with a range of cooling rates, are combined to test the capability of the FROST framework. The first dataset, referred to as PICOLITRE, is taken from Murray et al. (2011). In their experiments micron sized droplets containing known amounts of kaolinite (KGa-1b, Clay Mineral Society) mineral dust and supported on a hydrophobic surface, were

Representing time-dependent freezing behaviour

R. J. Herbert et al.

Title Page

Abstract

Introduction

Conclusions

References

Tables

Figures

◀

▶

◀

▶

Back

Close

Full Screen / Esc

Printer-friendly Version

Interactive Discussion

cooled at constant rates on a cold stage coupled with an optical microscope. Each experiment was characterised by a specific cooling rate and weight fraction of mineral per droplet. For this study four datasets are used (experiments vii, viii, ix and xi in Murray et al., 2011) corresponding to cooling rates (weight fractions) of 5.4 (0.0034), 9.6 (0.01), 0.8 (0.01) and 5.1 (0.01) Kmin^{-1} , respectively. For the second experimental dataset, referred to as MICROLITRE, a different cold-stage instrument was used, which has been described previously (O’Sullivan et al., 2013; Whale et al., 2013). In this experiment ~ 40 droplets of 1 μL volume containing known amounts of the same kaolinite sample as Murray et al. (2011) (KGa-1b) were held on a hydrophobic surface and cooled at constant rates with freezing events recorded optically. Four experiments were performed at cooling rates of 0.1, 0.2, 0.5, and 1.0 Kmin^{-1} , each with weight fractions of 0.01.

Nucleation rate coefficients for the PICOLITRE and MICROLITRE experiments are shown in Fig. 4a. The larger droplets in the new MICROLITRE experiment contain significantly greater IN surface area per droplet than the PICOLITRE experiment, which increases the probability of freezing, resulting in higher freezing temperatures. The nucleation rate coefficients plotted in Fig. 4a are derived using Eq. (1), hence the assumption in performing this analysis is that the species has a uniform IN distribution and behaves as a single-component system. At this stage we do not know if this assumption is valid, hence we specify that this is the apparent nucleation rate coefficient (J_{apparent}). In a single-component system a plot of $\ln(J_{\text{apparent}})$ vs. T will yield a slope equal to λ (recall that $\lambda = d\ln(J_i)/dT$), whereas if the system were multiple component then the slope of $\ln(J_{\text{apparent}})$ vs. T will be smaller than λ because an inappropriate model was used to derive J (i.e. $d\ln(J_{\text{apparent}})/dT$ is a lower limit to λ). For a set of data obtained at a single cooling rate it is impossible to say if the sample is single or multiple component, further tests are required. Murray et al. (2011) did this by performing isothermal experiments in addition to experiments at various cooling rates and showed that the values of J_{apparent} derived from both styles of experiment were consistent and concluded that nucleation by kaolinite KGa-1b was consistent with a single-component

system below 246 K and therefore $J_{\text{apparent}} = J_i$. We expand on this earlier analysis with additional data for kaolinite KGa-1b at warmer temperatures and place it in the context of the FROST framework. To test whether the MICROLITRE dataset is also consistent with a single-component system we performed an isothermal experiment, in addition to the experiments at various cooling rates.

The isothermal experiment, shown in Fig. 4b, was performed at 255.15 K with droplets containing a weight fraction 0.01 of KGa-1b particles. We have plotted the decay of liquid droplets expected based on the value of J at 255.15 ± 0.4 K determined from the linear fit to $\ln(J_{\text{apparent}})$ in Fig. 4a. The expected exponential decay matches the measured decay; this is consistent with a uniform species, and thus a single-component system. The derived J_{apparent} values from experiments at cooling rates ranging from 0.1 to 1.0 Kmin^{-1} are shown in Fig. 4a and also show consistency with this system.

In Fig. 5 we place the data from the cooling experiments in the context of FROST. If the IN species can be characterised with a single λ then the application of Eq. (19) will modify each data point by $T' = T_{\text{experiment}} - \beta(r)$. With the correct value of λ in the FROST framework, the data will converge onto the curve of a 1 Kmin^{-1} cooling experiment for the species tested. Figure 5a shows the fraction frozen curves and Fig. 5c shows $n_s(T)$ values, derived using Eq. (22) with a surface area calculated using a specific surface area of $11.8 \text{ m}^2 \text{ g}^{-1}$ (Murray et al., 2011). The $n_s(T)$ values depend on the cooling rate, with over a factor of five shift on changing the cooling rate by a factor of 10. On applying FROST with a λ of -1.12 (derived from $d\ln(J_{\text{apparent}})/dT$ in Fig. 4a) both the fraction frozen curves (Fig. 5b) and the $n_s(T')$ (Fig. 5d) converge. Again this supports the claim that kaolinite KGa-1b is well represented by a single-component system ($J_{\text{apparent}} = J_i$).

An interesting and potentially significant question is raised by this study of nucleation by kaolinite as the linear fit to the two independent datasets in Fig. 4a is made over 20 K which is at odds with CNT. CNT predict curvature in $\ln J$ vs. T over 10's of kelvin (Pruppacher, 1995). This might suggest that there is a flaw in CNT theory, or alternatively it may be the case that there are multiple IN populations which happen to

Representing time-dependent freezing behaviour

R. J. Herbert et al.

Title Page

Abstract

Introduction

Conclusions

References

Tables

Figures

◀

▶

◀

▶

Back

Close

Full Screen / Esc

Printer-friendly Version

Interactive Discussion



give the appearance of a single-component system. However, the evidence presented here suggests that KGa-1b behaves as a single component, with consistent behaviour at high and low temperatures. This issue requires further study to understand this potentially important finding, but is beyond the focus of this paper.

4.2 K-feldspar data from cold-stage instrument

In this example we investigate and determine the cooling-rate dependence of K-feldspar using the microlitre droplet instrument as in the previous example. K-feldspar was recently shown to be the most important mineral component of desert dusts for ice nucleation (Atkinson et al., 2013). In these experiments ~ 40 droplets of $1 \mu\text{L}$ volume, each containing a weight fraction 0.001 of K-feldspar, were cooled at constant rates of 0.2, 0.4, 1.0 and 2.0 Kmin^{-1} on a hydrophobic surface. The experimental fraction frozen data are shown in Fig. 6c. For the 0.2, 0.4 and 2.0 Kmin^{-1} curves two separate experiments were performed and for the 1.0 Kmin^{-1} curve five experiments were performed. A systematic shift in the fraction frozen curves outside of instrumental error ($\pm 0.4 \text{ K}$) can be seen for the experiments at 0.2 and 2 Kmin^{-1} , which indicates that there is a cooling-rate dependence for nucleation by K-feldspar.

We now need to test if this data is consistent with a single or multiple-component system. Nucleation rate coefficients, J_{apparent} , for the 0.2 and 2.0 Kmin^{-1} runs are shown in Fig. 6a (calculated using a specific surface area of $1.86 \text{ m}^2 \text{ g}^{-1}$, Whale et al., 2013). If K-feldspar behaved as a single-component system then the two datasets would fall onto the same line, as they do for kaolinite in Fig. 4a. However, they do not fall on the same line; the J_{apparent} values are significantly different between the two cooling rates, hence this suggests that K-feldspar is a diverse species and requires a multiple-component model to describe its freezing behaviour. In this case Eq. (1) should not be used to derive values of nucleation rate coefficients since $J_{\text{apparent}} \neq J_i$.

As stated in the previous section, with the correct value of λ in the FROST framework, the modified data will converge onto a single curve. Therefore, in order to determine

Title Page

Abstract

Introduction

Conclusions

References

Tables

Figures

◀

▶

◀

▶

Back

Close

Full Screen / Esc

Printer-friendly Version

Interactive Discussion



Representing time-dependent freezing behaviour

R. J. Herbert et al.

Title Page

Abstract

Introduction

Conclusions

References

Tables

Figures

⏪

⏩

◀

▶

Back

Close

Full Screen / Esc

Printer-friendly Version

Interactive Discussion



the value of λ , a procedure was followed where λ was iteratively varied until $n_s(T')$ converged onto a single curve (using Eq. 19). The best fit was determined by minimisation of the root-mean-square differences between the data and an exponential fit to $\ln(n_s)$. This fitting procedure resulted in $\lambda = -3.4$ and is shown in Fig. 6b. This value is significantly steeper than the gradients $d\ln(J_{\text{apparent}})/dT$ in Fig. 6a (0.85 and 0.9 K^{-1}). Recall that for kaolinite, the gradient $d\ln(J_{\text{apparent}})/dT$ was used to normalise the n_s values in Fig. 5d indicating that kaolinite is a uniform species. In K-feldspar the fact that $d\ln(J_{\text{apparent}})/dT \neq \lambda$ (where $\lambda = d\ln(J_i)/dT$) shows that K-feldspar exhibits a diverse nucleating ability across the population.

An isothermal experiment was also performed at $T_{\text{iso}} = 262.15\text{ K}$ with 20 droplets (28 froze during cooling to T_{iso}) containing a weight fraction 0.001 K-feldspar (see Fig. 7). For a uniform species the decay of liquid droplets over time will be exponential (as was the case for kaolinite KGa-1b in Fig. 4b), whereas a diverse species will result in a non-exponential decay. Inspection of the data in Fig. 7 shows that the decay of liquid droplets was not exponential, again consistent with a diverse population of IN. To highlight this, we have plotted the decay expected from the two limiting values of J_{apparent} from Fig. 6a at 262.15 K. The simulated decays, assuming a single-component system, clearly over predict freezing. We also simulate what we would expect for a diverse population where we use the MCSM to produce the expected decay of droplets. The MCSM was initially used as a fitting tool to obtain a distribution that best reproduced the entire normalised fraction frozen dataset in Fig. 6d, using the minimised value $\lambda = -3.4\text{ K}$ determined previously. This distribution ($\mu = 3.8$; $\sigma = 890.5$) was then used to simulate an isothermal experiment. These simulations included the initial cooling period required to reach the supercooled temperature. There is clear consistency between the diverse simulation and the experimental data. This again shows strong evidence that the K-feldspar sample used is a diverse species and would require a multiple-component system to describe its freezing behaviour.

This example is important as it illustrates that for a diverse IN species with multiple active components, the observed gradient of the derived n_s or J_{apparent} values from

a single experiment does not characterise its stochastic behaviour. For these species a series of experiments at different cooling rates or residence times must be performed in order to determine the value of λ that can be used to characterise its stochastic behaviour.

4.3 Mineral dust freezing experiments from the Zurich Ice Nucleation Chamber (ZINC)

Welti et al. (2012) (hereafter WELTI) studied the dependence of freezing probability on residence time for droplets containing particles of mineral dust using the ZINC continuous flow diffusion chamber. The mineral dust used by WELTI was supplied by the chemical company Fluka as kaolinite, but contained a range of minerals including feldspar and it has been suggested that it is this feldspar content which controls its ice nucleating ability (Atkinson et al., 2013). In their experiment, WELTI size-selected single particles, immersed them in supercooled droplets and passed the droplets into the ZINC instrument. Within ZINC the droplets experienced isothermal conditions and the frozen fraction was determined using a depolarization detector. Variable flow rates and a series of detection points provide a range of residence times, and by performing experiments at several temperature WELTI built up $f(T)$ curves for a range of residence times. For this study we use the data for 400 nm particles and the data is shown in Fig. 8a.

Each data point represents a single isothermal experiment with a single residence time, t . Hence, Eq. (20) can be used to modify each data point with $T' = T_{\text{experiment}} - \beta(t)$, assuming that the species can be characterised by a single value for λ . In order to determine the value of λ that describes the residence-time dependence, the same procedure was followed as in Sect. 4.2 for K-feldspar. Using derived $n_s(T)$ values, with each IN surface area based on a spherical particle 400 nm in diameter as per the experiment, λ was varied until the $n_s(T')$ values converged onto a single line, again described by an exponential fit to $\ln(n_s)$. This resulted in $\lambda_{\text{WELTI}} = -2.18$ with a $\ln(n_s)$ root-mean-square-error (RMSE) of 0.047, and is shown in Fig. 8b. For comparison,

Representing time-dependent freezing behaviour

R. J. Herbert et al.

Title Page

Abstract

Introduction

Conclusions

References

Tables

Figures



Back

Close

Full Screen / Esc

Printer-friendly Version

Interactive Discussion



an exponential fit describing the raw $n_s(T')$ data resulted in a RMSE of 0.076. The two exponential fits were used to reproduce the expected fraction frozen data for a 1 K min^{-1} cooling experiment, and are plotted along with the observed and normalised fraction frozen dataset in Fig. 8c and Fig. 8d respectively. Here the FROST framework has been used to both normalise isothermal experiments performed over a range of residence times, and determine a value of λ that can be used to potentially describe the cooling-rate and time-dependent behaviour of this mineral dust in simulations.

4.4 Volcanic ash from ZINC and AIDA

In this final example the framework is used to normalise droplet freezing data from two fundamentally different experimental methods. Following the eruption of Eyjafjallajökull in Iceland during April 2010, a single sample of volcanic ash was collected and analysed to investigate its freezing characteristics in the AIDA expansion chamber (Steinke et al., 2011, hereafter STEINKE) and the ZINC ice nucleating chamber (Hoyle et al., 2011, hereafter HOYLE). The ZINC instrument, as described in the previous section, was used to determine the total fraction of droplets frozen over a range of temperatures ($230 \leq T \leq 247 \text{ K}$) with a residence time of 12 s at each temperature; each supercooled droplet contained a single immersed particle, which ranged from ~ 0.1 to $300 \mu\text{m}$ in diameter, D . The 84 m^3 AIDA cloud chamber is capable of simulating an ascending, cooling air parcel, and is coupled to an array of instruments, which were used to determine the freezing characteristics of the same volcanic ash sample; in this method the dust sample ($\sim 0.1 \leq D \leq \sim 15 \mu\text{m}$) is dispersed into the cloud chamber prior to expansion.

The ice nucleating efficiencies of the two datasets were compared in Murray et al. (2012) and the subsequent n_s values are reproduced in Fig. 9a. It is clear that the two datasets, albeit with similar gradients, do not show good agreement even though the same sample was used.

Representing time-dependent freezing behaviour

R. J. Herbert et al.

Title Page

Abstract

Introduction

Conclusions

References

Tables

Figures



Back

Close

Full Screen / Esc

Printer-friendly Version

Interactive Discussion



time can be seen as an equivalent shift in temperature along the function describing the nucleation rate. This function is exponential and therefore can have a significant effect on the resulting freezing probability.

A first-order indication of the potential importance of time-dependence is shown in Fig. 10 where values of β_{cool} and β_{iso} for $-0.1 \geq \lambda \geq -10$ have been plotted. Each point represents the shift of a specific fraction frozen, by a temperature βK , that results from a fractional change in either cooling-rate or residence-time for a species with a specific value of λ (as per Eqs. 8 and 9). This plot shows how materials with a smaller absolute value of λ are more sensitive to timescale with larger shifts in β for the same change in timescale.

The four IN species that were used as examples in Sect. 4 have been included in Fig. 10 and show that this selection of atmospherically relevant species exhibits a range of time-dependent behaviour. IN species that have a value of λ with a large magnitude ($|\lambda| > 5$) will exhibit very little time-dependence and would likely be well approximated by a singular freezing model. For those with a small magnitude (especially $|\lambda| < 1$, such as the volcanic ash from HOYLE and STEINKE) the significant cooling-rate and residence-time dependence must be taken into account. This finding is important because it changes the way we should frame the debate of whether time-dependence is important in ice nucleation. In the past the question has been whether time-dependence is important, but this question should be rephrased to whether a particular IN species has a strong time-dependence or not, and at what point this stops having an impact on ice nucleation rates, i.e. is there a limiting value of $|\lambda|$, beyond which the singular freezing model is adequate?

5.2 Representing complex IN populations in cloud models

The range in time-dependent behaviour shown for the IN in Sect. 4 leads to the question of how to best implement this behaviour for a complex multiple-component IN sample, or population, where each component has a characteristic time-dependence, within a cloud model.

Representing time-dependent freezing behaviour

R. J. Herbert et al.

Title Page

Abstract

Introduction

Conclusions

References

Tables

Figures

◀

▶

◀

▶

Back

Close

Full Screen / Esc

Printer-friendly Version

Interactive Discussion



Representing time-dependent freezing behaviour

R. J. Herbert et al.

Title Page

Abstract

Introduction

Conclusions

References

Tables

Figures

◀

▶

◀

▶

Back

Close

Full Screen / Esc

Printer-friendly Version

Interactive Discussion



The time-dependence of a population of IN containing many separate species may be dominated by a single component, and therefore a single value or temperature dependent function of λ . Where distinct components are dominant in different temperature ranges it would be possible to have a temperature dependent function of λ to reflect the relative dominance of each component. For multiple-species aerosol where no single component is observably dominant, the population of particles/droplets would need to be split into separate components and treated as an externally mixed population.

Several ice nucleation schemes have been developed that incorporate multiple components in order to improve the treatment of IN populations in models: Diehl and Wurzler (2010) used a simple fractional occurrence factor to model potential immersion mode droplets containing bacterial, mineral and soot IN; Phillips et al. (2008) used classifications of dust/metallic, black carbon and organic aerosols in a similar method for modelling a population of IN species; and Barahona (2012) introduced the ice nucleation spectrum framework, capable of relating different aerosol properties to ice nucleation in the deposition mode, with the potential to extend to immersion freezing.

Whilst these models are capable of describing separate species it may be more realistic to represent a series of dominant components so that the time-dependence and inter-particle variability can be accurately described for a complex, evolving IN population. To achieve this, the λ characterisation of each component needs to be determined through a series of isothermal and cooling experiments on IN samples that have very high purities. Commonly tested samples, such as ATD and Illite, are comprised of several mineralogical components and may therefore contain multiple IN species. Once λ has been determined for the individual or dominant component of the species then the normalised data can be used with the FROST framework.

6 Conclusions

The range of instruments and techniques that are used for characterising the freezing properties of IN species result in different temporal conditions, i.e. CFDC instruments

routinely use a constant temperature and residence time, whereas cold stage instruments and cloud chambers typically cool droplets at some rate to determine freezing behaviour. Taking into account the differences in timescale between these experiments and translating this information to cloud formation in the atmosphere has been a challenge.

In this study we have developed a new framework to address this challenge. This framework is underpinned by the finding that the temperature shift observed on changing cooling rate is directly related to the slope $d\ln(J_i)/dT$ (λ). We also extended this relationship to freezing experiments conducted under isothermal conditions with varying residence times. We refer to this framework as the Framework for Reconciling Observable Stochastic Time-dependence (FROST) and use it in combination with the singular freezing model. Therefore the FROST framework can be used to describe both the inter-particle variability and the stochastic nature of ice nucleation within a simple parameterisation.

To test the FROST framework, data obtained from a variety of instruments (including the ZINC flow chamber, AIDA expansion chamber and two cold-stage instruments) were analysed to determine the value for λ that best described the observed time-dependence of each species. It is striking that the parameter λ depends strongly on the material, with feldspar having the largest magnitude, and the weakest time-dependence, and volcanic ash having the smallest magnitude, with the strongest time-dependence. More work is needed in order to quantify λ for other atmospherically relevant ice nuclei.

Supplementary material related to this article is available online at
**[http://www.atmos-chem-phys-discuss.net/14/1399/2014/
acpd-14-1399-2014-supplement.pdf](http://www.atmos-chem-phys-discuss.net/14/1399/2014/acpd-14-1399-2014-supplement.pdf)**

Acknowledgements. We thank A. Welti for kindly providing the kaolinite (K-SA) dataset and D. O'Sullivan for helpful discussions. We gratefully acknowledge the European Research Coun-

**Representing
time-dependent
freezing behaviour**

R. J. Herbert et al.

Title Page

Abstract

Introduction

Conclusions

References

Tables

Figures



Back

Close

Full Screen / Esc

Printer-friendly Version

Interactive Discussion



cil (FP7, 240449 ICE) and the Natural Environment Research Council (NE/I019057/1) for funding.

References

5 Abbatt, J. P. D. and Nowak, J. B.: Heterogeneous interactions of HBr and HOCl with cold sulfuric acid solutions: Implications for arctic boundary layer bromine chemistry, *J. Phys. Chem. A*, 101, 2131–2137, doi:10.1021/Jp963117b, 1997.

Ansmann, A., Mattis, I., Müller, D., Wandinger, U., Radlach, M., Althausen, D., and Damoah, R.: Ice formation in Saharan dust over central Europe observed with temperature/humidity/aerosol Raman lidar, *J. Geophys. Res.-Atmos.*, 110, D18S12, doi:10.1029/2004jd005000, 2005.

10 Ansmann, A., Tesche, M., Seifert, P., Althausen, D., Engelmann, R., Fruntke, J., Wandinger, U., Mattis, I., and Müller, D.: Evolution of the ice phase in tropical altocumulus: SAMUM lidar observations over Cape Verde, *J. Geophys. Res.*, 114, D17208, doi:10.1029/2008jd011659, 2009.

15 Atkinson, J. D., Murray, B. J., Woodhouse, M. T., Whale, T. F., Baustian, K. J., Carslaw, K. S., Dobbie, S., O'Sullivan, D., and Malkin, T. L.: The importance of feldspar for ice nucleation by mineral dust in mixed-phase clouds, *Nature*, 498, 355–358, doi:10.1038/nature12278, 2013.

Barahona, D.: On the ice nucleation spectrum, *Atmos. Chem. Phys.*, 12, 3733–3752, doi:10.5194/acp-12-3733-2012, 2012.

20 Broadley, S. L., Murray, B. J., Herbert, R. J., Atkinson, J. D., Dobbie, S., Malkin, T. L., Condliffe, E., and Neve, L.: Immersion mode heterogeneous ice nucleation by an illite rich powder representative of atmospheric mineral dust, *Atmos. Chem. Phys.*, 12, 287–307, doi:10.5194/acp-12-287-2012, 2012.

25 Conen, F., Morris, C. E., Leifeld, J., Yakutin, M. V., and Alewell, C.: Biological residues define the ice nucleation properties of soil dust, *Atmos. Chem. Phys.*, 11, 9643–9648, doi:10.5194/acp-11-9643-2011, 2011.

Connolly, P. J., Möhler, O., Field, P. R., Saathoff, H., Burgess, R., Choularton, T., and Gallagher, M.: Studies of heterogeneous freezing by three different desert dust samples, *Atmos. Chem. Phys.*, 9, 2805–2824, doi:10.5194/acp-9-2805-2009, 2009.

ACPD

14, 1399–1442, 2014

Representing time-dependent freezing behaviour

R. J. Herbert et al.

Title Page

Abstract

Introduction

Conclusions

References

Tables

Figures

◀

▶

◀

▶

Back

Close

Full Screen / Esc

Printer-friendly Version

Interactive Discussion



**Representing
time-dependent
freezing behaviour**

R. J. Herbert et al.

Title Page

Abstract

Introduction

Conclusions

References

Tables

Figures

◀

▶

◀

▶

Back

Close

Full Screen / Esc

Printer-friendly Version

Interactive Discussion



Cui, Z., Carslaw, K. S., Yin, Y., and Davies, S.: A numerical study of aerosol effects on the dynamics and microphysics of a deep convective cloud in a continental environment, *J. Geophys. Res.*, 111, D05201, doi:10.1029/2005jd005981, 2006.

Cziczo, D. J., Stetzer, O., Worringer, A., Ebert, M., Weinbruch, S., Kamphus, M., Gallavardin, S. J., Curtius, J., Borrmann, S., Froyd, K. D., Mertes, S., Mohler, O., and Lohmann, U.: Inadvertent climate modification due to anthropogenic lead, *Nat. Geosci.*, 2, 333–336, doi:10.1038/Ngeo499, 2009.

de Boer, G., Morrison, H., Shupe, M. D., and Hildner, R.: Evidence of liquid dependent ice nucleation in high-latitude stratiform clouds from surface remote sensors, *Geophys. Res. Lett.*, 38, L01803, doi:10.1029/2010gl046016, 2011.

DeMott, P. J.: Quantitative descriptions of ice formation mechanisms of silver iodide-type aerosols, *Atmos. Res.*, 38, 63–99, 1995.

Diehl, K. and Wurzler, S.: Air parcel model simulations of a convective cloud: bacteria acting as immersion ice nuclei, *Atmos. Environ.*, 44, 4622–4628, doi:10.1016/j.atmosenv.2010.08.003, 2010.

Dobbie, S. and Jonas, P. R.: Radiative influences on the structure and lifetime of cirrus clouds, *Q. J. Roy. Meteor. Soc.*, 127, 2663–2682, doi:10.1256/Smsqj.57807, 2001.

Ervens, B. and Feingold, G.: Sensitivities of immersion freezing: reconciling classical nucleation theory and deterministic expressions, *Geophys. Res. Lett.*, 40, 3320–3324, doi:10.1002/grl.50580, 2013.

Field, P. R., Heymsfield, A. J., Shipway, B. J., DeMott, P. J., Pratt, K. A., Rogers, D. C., Stith, J., and Prather, K. A.: Ice in Clouds Experiment–Layer Clouds, Part II: testing characteristics of heterogeneous ice formation in lee wave clouds, *J. Atmos. Sci.*, 69, 1066–1079, doi:10.1175/jas-d-11-026.1, 2012.

Hartmann, D. L., Ockert-Bell, M. E., and Michelsen, M. L.: The effect of cloud type on earth's energy balance: global analysis, *J. Climate*, 5, 1281–1304, doi:10.1175/1520-0442(1992)005<1281:teocto>2.0.co;2, 1992.

Hoose, C. and Möhler, O.: Heterogeneous ice nucleation on atmospheric aerosols: a review of results from laboratory experiments, *Atmos. Chem. Phys.*, 12, 9817–9854, doi:10.5194/acp-12-9817-2012, 2012.

Hoyle, C. R., Pinti, V., Welti, A., Zobrist, B., Marcolli, C., Luo, B., Höskuldsson, Á., Mattsson, H. B., Stetzer, O., Thorsteinsson, T., Larsen, G., and Peter, T.: Ice nucleation properties

**Representing
time-dependent
freezing behaviour**

R. J. Herbert et al.

Title Page

Abstract

Introduction

Conclusions

References

Tables

Figures

◀

▶

◀

▶

Back

Close

Full Screen / Esc

Printer-friendly Version

Interactive Discussion



of volcanic ash from Eyjafjallajökull, *Atmos. Chem. Phys.*, 11, 9911–9926, doi:10.5194/acp-11-9911-2011, 2011.

Kashchiev, D., Borissova, A., Hammond, R. B., and Roberts, K. J.: Effect of cooling rate on the critical undercooling for crystallization, *J. Cryst. Growth*, 312, 698–704, 2009.

5 Kulkarni, G. and Dobbie, S.: Ice nucleation properties of mineral dust particles: determination of onset RH_i , IN active fraction, nucleation time-lag, and the effect of active sites on contact angles, *Atmos. Chem. Phys.*, 10, 95–105, doi:10.5194/acp-10-95-2010, 2010.

Ladino, L., Stetzer, O., Lüönd, F., Welti, A., and Lohmann, U.: Contact freezing experiments of kaolinite particles with cloud droplets, *J. Geophys. Res.-Atmos.*, 116, D22202, doi:10.1029/2011jd015727, 2011.

10 Ladino Moreno, L. A., Stetzer, O., and Lohmann, U.: Contact freezing: a review of experimental studies, *Atmos. Chem. Phys.*, 13, 9745–9769, doi:10.5194/acp-13-9745-2013, 2013.

Lau, K. M. and Wu, H. T.: Warm rain processes over tropical oceans and climate implications, *Geophys. Res. Lett.*, 30, 2290, doi:10.1029/2003gl018567, 2003.

15 Levine, J.: Statistical Explanation of Spontaneous Freezing of Water Droplets, NACA Tech. Note, 2234, 1950

Lüönd, F., Stetzer, O., Welti, A., and Lohmann, U.: Experimental study on the ice nucleation ability of size-selected kaolinite particles in the immersion mode, *J. Geophys. Res.*, 115, D14201, doi:10.1029/2009jd012959, 2010.

20 Marcolli, C., Gedamke, S., Peter, T., and Zobrist, B.: Efficiency of immersion mode ice nucleation on surrogates of mineral dust, *Atmos. Chem. Phys.*, 7, 5081–5091, doi:10.5194/acp-7-5081-2007, 2007.

Murray, B. J., Broadley, S. L., Wilson, T. W., Bull, S. J., Wills, R. H., Christenson, H. K., and Murray, E. J.: Kinetics of the homogeneous freezing of water, *Phys. Chem. Chem. Phys.*, 12, 10380–10387, doi:10.1039/c003297b, 2010.

25 Murray, B. J., Broadley, S. L., Wilson, T. W., Atkinson, J. D., and Wills, R. H.: Heterogeneous freezing of water droplets containing kaolinite particles, *Atmos. Chem. Phys.*, 11, 4191–4207, doi:10.5194/acp-11-4191-2011, 2011.

Murray, B. J., O’Sullivan, D., Atkinson, J. D., and Webb, M. E.: Ice nucleation by particles immersed in supercooled cloud droplets, *Chem Soc Rev*, 41, 6519–6554, doi:10.1039/c2cs35200a, 2012.

30 Niedermeier, D., Shaw, R. A., Hartmann, S., Wex, H., Clauss, T., Voigtländer, J., and Stratmann, F.: Heterogeneous ice nucleation: exploring the transition from stochastic to singu-

Representing
time-dependent
freezing behaviour

R. J. Herbert et al.

Title Page

Abstract

Introduction

Conclusions

References

Tables

Figures

◀

▶

◀

▶

Back

Close

Full Screen / Esc

Printer-friendly Version

Interactive Discussion



- lar freezing behavior, *Atmos. Chem. Phys.*, 11, 8767–8775, doi:10.5194/acp-11-8767-2011, 2011.
- O'Sullivan, D., Murray, B. J., Malkin, T. L., Whale, T., Umo, N. S., Atkinson, J. D., Price, H. C., Baustian, K. J., Browse, J., and Webb, M. E.: Ice nucleation by soil dusts: relative importance of mineral dust and biogenic components, *Atmos. Chem. Phys. Discuss.*, 13, 20275–20317, doi:10.5194/acpd-13-20275-2013, 2013.
- Phillips, V. T. J., DeMott, P. J., and Andronache, C.: An empirical parameterization of heterogeneous ice nucleation for multiple chemical species of aerosol, *J. Atmos. Sci.*, 65, 2757–2783, doi:10.1175/2007JAS2546.1, 2008.
- Pruppacher, H. R.: A new look at homogeneous ice nucleation in supercooled water drops, *J. Atmos. Sci.*, 52, 1924–1933, doi:10.1175/1520-0469(1995)052<1924:ANLAHI>2.0.CO;2, 1995.
- Pruppacher, H. R. and Klett, J. D.: *Microphysics of Clouds and Precipitation*, 2 edn., Kulwer Academic Publishers, Dordrecht, 1997.
- Sassen, K. and Khvorostyanov, V. I.: Microphysical and radiative properties of mixed-phase altocumulus: a model evaluation of glaciation effects, *Atmos. Res.*, 84, 390–398, doi:10.1016/j.atmosres.2005.08.017, 2007.
- Sear, R. P.: Generalisation of Levine's prediction for the distribution of freezing temperatures of droplets: a general singular model for ice nucleation, *Atmos. Chem. Phys.*, 13, 7215–7223, doi:10.5194/acp-13-7215-2013, 2013.
- Stan, C. A., Schneider, G. F., Shevkopyas, S. S., Hashimoto, M., Ibanescu, M., Wiley, B. J., and Whitesides, G. M.: A microfluidic apparatus for the study of ice nucleation in supercooled water drops, *Lab Chip*, 9, 2293–2305, doi:10.1039/b906198c, 2009.
- Steinke, I., Möhler, O., Kiselev, A., Niemand, M., Saathoff, H., Schnaiter, M., Skrotzki, J., Hoose, C., and Leisner, T.: Ice nucleation properties of fine ash particles from the Eyjafjallajökull eruption in April 2010, *Atmos. Chem. Phys.*, 11, 12945–12958, doi:10.5194/acp-11-12945-2011, 2011.
- Vali, G.: Quantitative Evaluation of Experimental Results an the Heterogeneous Freezing Nucleation of Supercooled Liquids, *J. Atmos. Sci.*, 28, 402–409, doi:10.1175/1520-0469(1971)028<0402:QEOERA>2.0.CO;2, 1971.
- Vali, G.: Nucleation terminology, *J. Aerosol Sci.*, 16, 575–576, doi:10.1016/0021-8502(85)90009-6, 1985.

**Representing
time-dependent
freezing behaviour**

R. J. Herbert et al.

Title Page

Abstract

Introduction

Conclusions

References

Tables

Figures

◀

▶

◀

▶

Back

Close

Full Screen / Esc

Printer-friendly Version

Interactive Discussion



- Vali, G.: Freezing rate due to heterogeneous nucleation, *J. Atmos. Sci.*, 51, 1843–1856, doi:10.1175/1520-0469(1994)051<1843:FRDTHN>2.0.CO;2, 1994.
- Vali, G.: Repeatability and randomness in heterogeneous freezing nucleation, *Atmos. Chem. Phys.*, 8, 5017–5031, doi:10.5194/acp-8-5017-2008, 2008.
- 5 Vali, G. and Stansbury, E. J.: Time-Dependent characteristics of the heterogeneous nucleation of ice, *Can. J. Phys.*, 44, 477–502, doi:10.1139/p66-044, 1966.
- Welti, A., Lüönd, F., Kanji, Z. A., Stetzer, O., and Lohmann, U.: Time dependence of immersion freezing: an experimental study on size selected kaolinite particles, *Atmos. Chem. Phys.*, 12, 9893–9907, doi:10.5194/acp-12-9893-2012, 2012.
- 10 Westbrook, C. D. and Illingworth, A. J.: The formation of ice in a long-lived supercooled layer cloud, *Q. J. Roy. Meteor. Soc.*, 139, 2209–2221, doi:10.1002/qj.2096, 2013.
- Whale, T. F., Murray, B. J., O'Sullivan, D., Umo, N. S., Baustian, K. J., Atkinson, J. D., and Morris, G. J.: A technique for quantifying rare ice nucleation events, *Atmos. Meas. Tech. Discuss.*, in preparation, 2013.
- 15 Wilson, P. W. and Haymet, A. D. J.: The spread of nucleation temperatures of a sample of supercooled liquid is independent of the average nucleation temperature, *J. Phys. Chem. B*, 116, 13472–13475, doi:10.1021/jp308177b, 2012.
- Wright, T. P. and Petters, M. D.: The role of time in heterogeneous freezing nucleation, *J. Geophys. Res.-Atmos.*, 118, 3731–3743, doi:10.1002/jgrd.50365, 2013.
- 20 Zhang, D., Wang, Z., and Liu, D.: A global view of midlevel liquid-layer topped stratiform cloud distribution and phase partition from CALIPSO and CloudSat measurements, *J. Geophys. Res.-Atmos.*, 115, D00H13, doi:10.1029/2009jd012143, 2010.

Representing time-dependent freezing behaviour

R. J. Herbert et al.

Table 1. The range of MCSM variables used for droplet cooling simulations in Fig. 3: λ is $d\ln(J_i)/dT$; μ and σ are the mean and standard deviation of the PDF used to constrain the occurrence of each component with “formula” referring to $\mu = -\lambda 240 + 14.8$; surface area of immersed IN per droplet s ; and the fraction f at which the change in temperature ($\Delta T = T(f_{r_1}) - T(f_{r_2})$) for a change in cooling rate r is calculated. All simulations were performed at cooling rates of 1 and 10 K min^{-1} .

Gradient λ	PDF mean μ	PDF width σ	Surface area s	Fraction f
$0.2 \leq -\lambda \leq 14$	formula	1	$1 \times 10^{-7} \text{ cm}^2$	0.5
$0.1 \leq -\lambda \leq 16$	formula	0.1	$5 \times 10^{-7} \text{ cm}^2$	0.5
$0.04 \leq -\lambda \leq 10$	formula	1	$10 \times 10^{-7} \text{ cm}^2$	0.25
$1 \leq -\lambda \leq 16$	formula	5	$1 \times 10^{-7} \text{ cm}^2$	0.25
$2 \leq -\lambda \leq 16$	formula + 10	10	$1 \times 10^{-7} \text{ cm}^2$	0.75
$0.02 \leq -\lambda \leq 0.1$	formula	1	$1 \times 10^{-7} \text{ cm}^2$	0.1
0.03	$\mu_1 = 9, \mu_2 = 12$	$\sigma_1 = 0.1, \sigma_2 = 2$	$1 \times 10^{-7} \text{ cm}^2$	0.5
1.0	$\mu_1 = 255, \mu_2 = 265$	$\sigma_1 = 1, \sigma_2 = 2$	$1 \times 10^{-7} \text{ cm}^2$	0.5
5.0	$\mu_1 = 1255, \mu_2 = 1260$	$\sigma_1 = 1, \sigma_2 = 5$	$1 \times 10^{-7} \text{ cm}^2$	0.5
10.0	$\mu_1 = 2455, \mu_2 = 2465, \mu_3 = 2460$	$\sigma_1 = 1, \sigma_2 = 1, \sigma_3 = 5$	$1 \times 10^{-7} \text{ cm}^2$	0.5

[Title Page](#)
[Abstract](#)
[Introduction](#)
[Conclusions](#)
[References](#)
[Tables](#)
[Figures](#)
[Back](#)
[Close](#)
[Full Screen / Esc](#)
[Printer-friendly Version](#)
[Interactive Discussion](#)


Representing time-dependent freezing behaviour

R. J. Herbert et al.

Title Page

Abstract

Introduction

Conclusions

References

Tables

Figures

◀

▶

◀

▶

Back

Close

Full Screen / Esc

Printer-friendly Version

Interactive Discussion

Table A1. Nomenclature.

Notation	Description
$J_i(T)$	The nucleation rate coefficient ($\text{cm}^{-2} \text{s}^{-1}$) for a single component i .
λ	The temperature dependence of the nucleation rate coefficient of a single component $d\ln(J_i)/dT$.
J_{apparent}	The apparent nucleation rate coefficient derived from experimental data using Eq. (1) and assuming a uniform IN species. If $\lambda = d\ln(J_{\text{apparent}})/dT$ then the species being tested is uniform and $J_{\text{apparent}} = J_i$, whereas if $\lambda \neq d\ln(J_{\text{apparent}})/dT$ then the species being tested is not uniform and $J_{\text{apparent}} \neq J_i$.
β	Systematic shift in temperature (K) of the fraction frozen $f(T)$ upon a temporal change.
$\beta(r)$	Systematic shift in temperature (K) of the fraction frozen $f(T)$ as a function of cooling rate (r) in Kmin^{-1} upon normalising to a cooling rate of 1Kmin^{-1} .
$\beta(t)$	Systematic shift in temperature (K) of the fraction frozen $f(T)$ as a function of residence-time (t) in seconds upon normalising to a cooling rate of 1Kmin^{-1} .
T'	The modified temperature of an experimentally determined data point normalised to a cooling experiment at 1Kmin^{-1} where $T' = T_{\text{experiment}} + \beta$.
$n_s(T)$	Nucleation coefficient, or ice active site density, (cm^{-2}) derived from experimental data using Eq. (22).
$n_s(T')$	Nucleation coefficient modified by a temperature β as above, thus normalising all data points to a cooling rate of 1Kmin^{-1} .
$d\ln(n_s)/dT'$	Temperature dependence of the nucleation coefficient. For a single-component system $d\ln(n_s)/dT' = \lambda$.

Representing time-dependent freezing behaviour

R. J. Herbert et al.

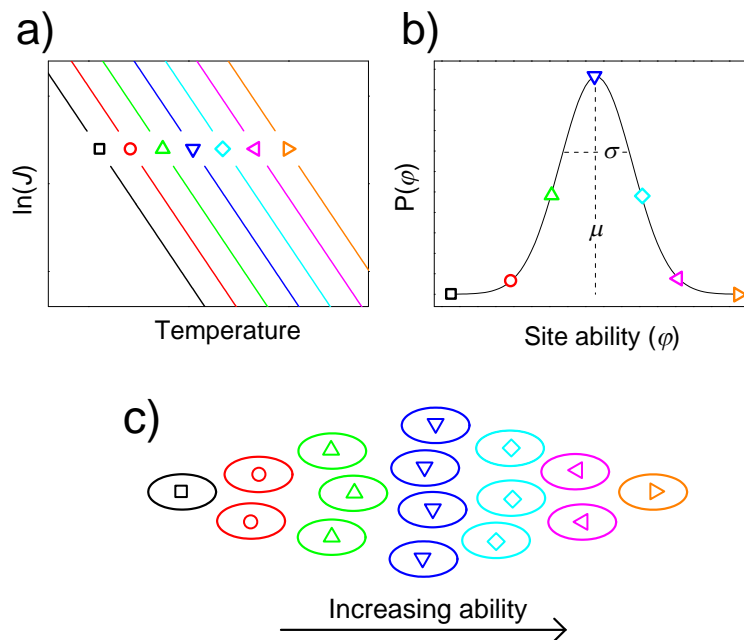


Fig. 1. Principles of the Multiple Component Stochastic Model. Each symbol represents a sub-population approximated by a single-component system, as shown in (a), with gradient $d\ln(J)/dT = \lambda$ and intercept φ (proxy for nucleating efficiency). The probability of occurrence for each component, characterised by φ , is determined using a statistical distribution, as depicted in (b), with a mean μ and standard deviation σ . Applying this probability to population of droplets results in an ensemble of droplets exhibiting a range of nucleating efficiencies as in (c).

[Title Page](#)
[Abstract](#)
[Introduction](#)
[Conclusions](#)
[References](#)
[Tables](#)
[Figures](#)
[◀](#)
[▶](#)
[◀](#)
[▶](#)
[Back](#)
[Close](#)
[Full Screen / Esc](#)
[Printer-friendly Version](#)
[Interactive Discussion](#)

Representing time-dependent freezing behaviour

R. J. Herbert et al.

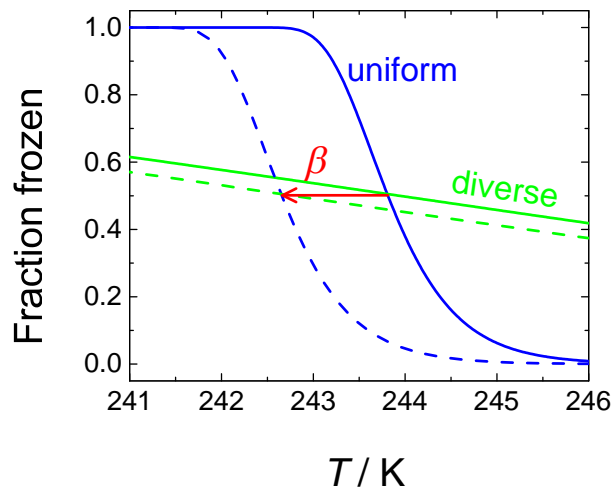


Fig. 2. Illustration of why the systematic shift in temperature (β) observed for a change in cooling rate is independent of the variability in ice nucleating ability. Cumulative fraction frozen curves shown are for a uniform ($\sigma = 0.01$) and diverse ($\sigma = 20$) IN population where $\lambda = -2$, and cooled at a constant rate of 1 K min^{-1} (solid line) and 10 K min^{-1} (dashed line). β corresponds to the shift in temperature (K) observed when 50% of droplets have frozen.

Title Page

Abstract

Introduction

Conclusions

References

Tables

Figures

◀

▶

◀

▶

Back

Close

Full Screen / Esc

Printer-friendly Version

Interactive Discussion



Representing time-dependent freezing behaviour

R. J. Herbert et al.

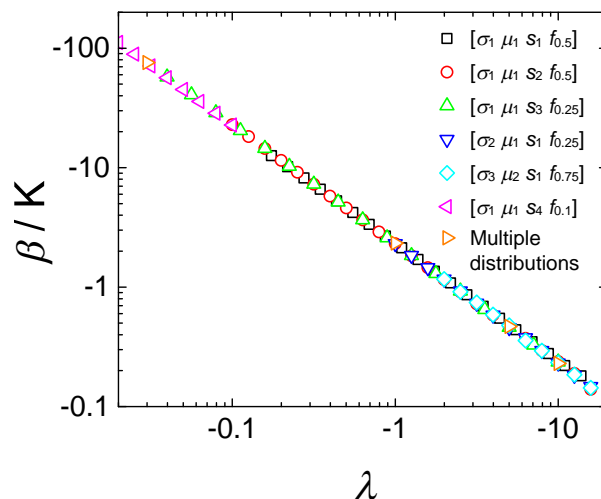


Fig. 3. A direct relationship between λ ($d\ln(J_i)/dT$) and β (the shift in freezing temperature upon a factor of 10 change in cooling rate) is observed for all droplet cooling simulations. For each set of runs λ was systematically increased whilst the following variables were set: mean (μ) and standard deviation (σ) of the PDF, surface area of particle per droplet (s), and the fraction at which the change in temperature was calculated (f). More information can be found in Table 1.

Title Page

Abstract

Introduction

Conclusions

References

Tables

Figures

◀

▶

◀

▶

Back

Close

Full Screen / Esc

Printer-friendly Version

Interactive Discussion



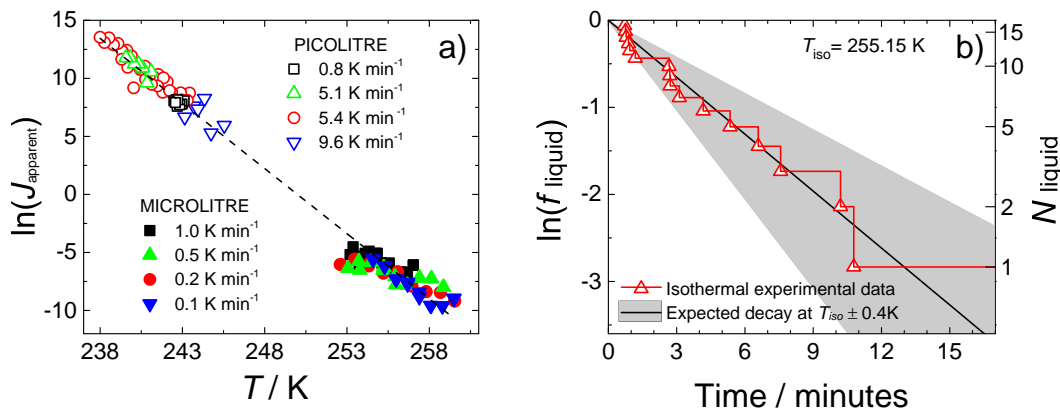


Fig. 4. Droplet freezing data for kaolinite (KGa-1b). **(a)** Shows nucleation rate coefficient (J_{apparent}) against temperature determined from droplet freezing experiments with a range of cooling rates. Open symbols represent PICOLITRE experiments from Murray et al. (2011) and closed symbols represent MICROLITRE experiments. Temperature uncertainty for the MICROLITRE data (not shown) is estimated at ± 0.4 K, and uncertainty in J (not shown) is estimated at -17% and $+25\%$. **(b)** Shows the exponential decay of liquid droplets during an isothermal experiment at 255.15 K together with a modelled experiment at the same temperature using the linear fit ($\ln(J) = -1.12T + 280.42$) shown in panel **(a)** as a dashed line. The grey area follows the experimental uncertainty in T around the modelled isothermal. The experiment duration was 17 min, at which point one droplet remained unfrozen.

Representing time-dependent freezing behaviour

R. J. Herbert et al.

Title Page

Abstract

Introduction

Conclusions

References

Tables

Figures

◀

▶

◀

▶

Back

Close

Full Screen / Esc

Printer-friendly Version

Interactive Discussion



Representing time-dependent freezing behaviour

R. J. Herbert et al.

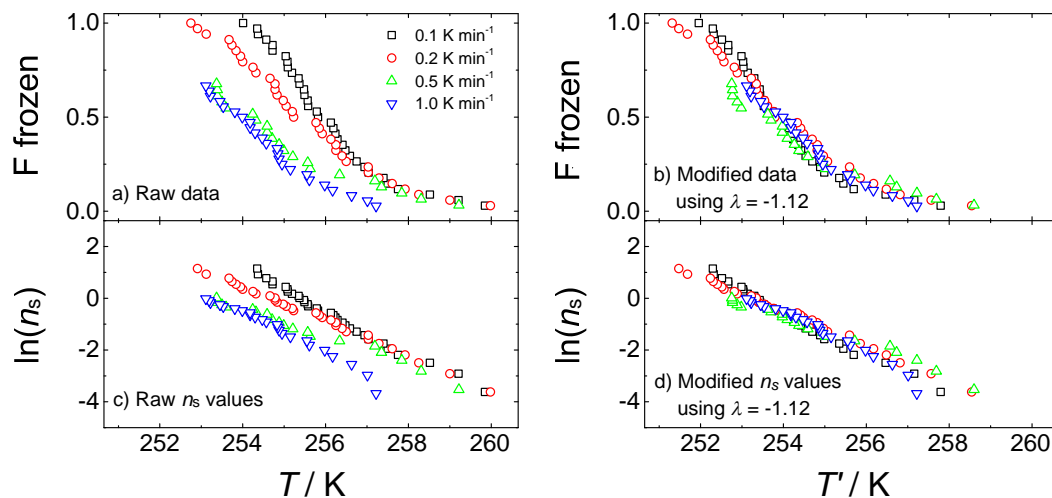


Fig. 5. Raw fraction frozen data and derived n_s values from kaolinite (KGA-1b) MICROLITRE cooling experiments ((a) and (c) respectively), and the normalised data ((b) and (d)) using the value of λ determined directly from the linear fit to $\ln(J)$ against T in Fig. 4a. Temperature and n_s uncertainty is as in Fig. 4.

Title Page

Abstract

Introduction

Conclusions

References

Tables

Figures

◀

▶

◀

▶

Back

Close

Full Screen / Esc

Printer-friendly Version

Interactive Discussion



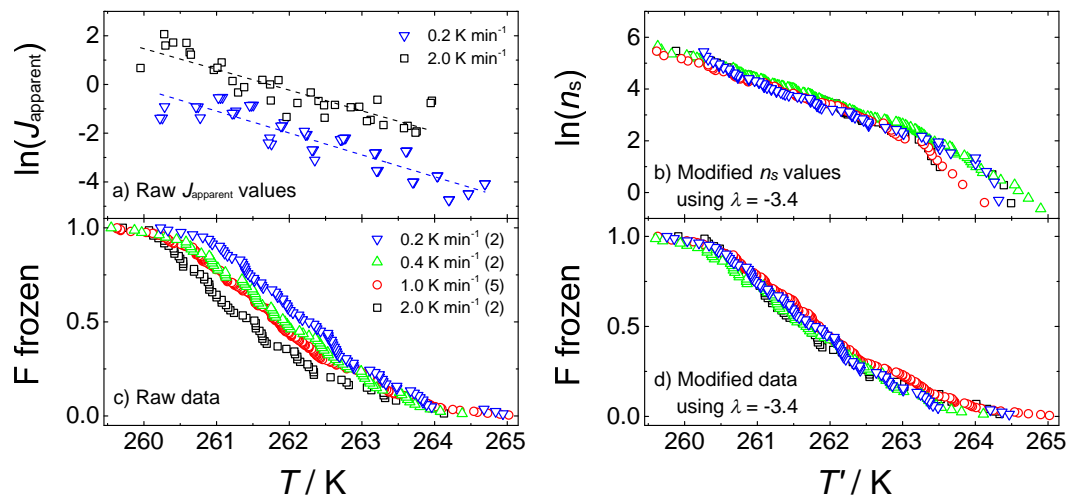


Fig. 6. Raw fraction frozen data and derived J_{apparent} and n_s values from K-feldspar MICROLITRE experiments. The consistent separation of $J_{\text{apparent}}(T)$ values at different cooling rates, shown in (a), suggest this IN species behaves as a multiple-component system. Due to this the apparent gradient of $d\ln(J_{\text{apparent}})/dT$ cannot be used to directly determine λ . Modified $n_s(T)$ data was minimised in order to determine a value of λ that best describes the cooling rate dependence, resulting in $\lambda = -3.4$. The raw and modified fraction frozen data is shown in (c) and (d) respectively. Temperature and n_s uncertainty is as in Fig. 4, and uncertainty in J (not shown) is estimated as roughly $\pm 15\%$.

Representing time-dependent freezing behaviour

R. J. Herbert et al.

Title Page

Abstract

Introduction

Conclusions

References

Tables

Figures

◀

▶

◀

▶

Back

Close

Full Screen / Esc

Printer-friendly Version

Interactive Discussion



Representing time-dependent freezing behaviour

R. J. Herbert et al.

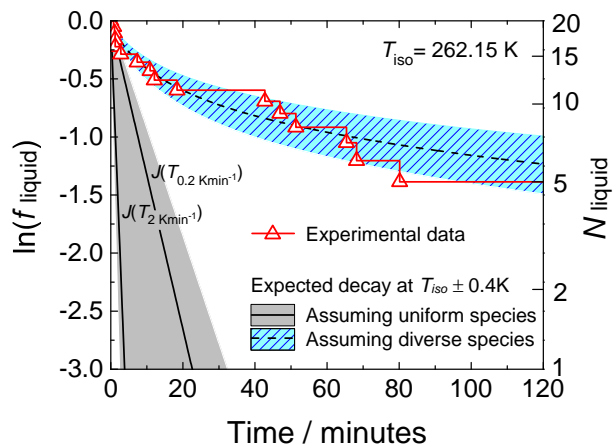


Fig. 7. Decay of liquid droplets in an isothermal experiment at $T_{\text{iso}} = 262.15$ K using K-feldspar, and simulated experiments assuming a uniform and diverse distribution. For the uniform distribution $J_{\text{apparent}}(T_{\text{iso}})$ values were taken from Fig. 6a and used with Eq. (1), resulting in a decay bounded by the range of J_{apparent} between the two cooling rates of 0.2 and 2.0 K min^{-1} . For the diverse simulation the MCSM was used with parameters determined through fitting to the normalised K-feldspar dataset in Fig. 6: $\mu = 890.5$, $\sigma = 3.8$ (see Fig. 1), and $\lambda = -3.4$ (determined in Fig. 6). The shaded regions follow the instrument-based error of ± 0.4 K around T_{iso} . The triangular symbols indicate when a freezing event occurred, throughout the 120 min duration of the experiment.

[Title Page](#)
[Abstract](#)
[Introduction](#)
[Conclusions](#)
[References](#)
[Tables](#)
[Figures](#)
[◀](#)
[▶](#)
[◀](#)
[▶](#)
[Back](#)
[Close](#)
[Full Screen / Esc](#)
[Printer-friendly Version](#)
[Interactive Discussion](#)


Representing
time-dependent
freezing behaviour

R. J. Herbert et al.

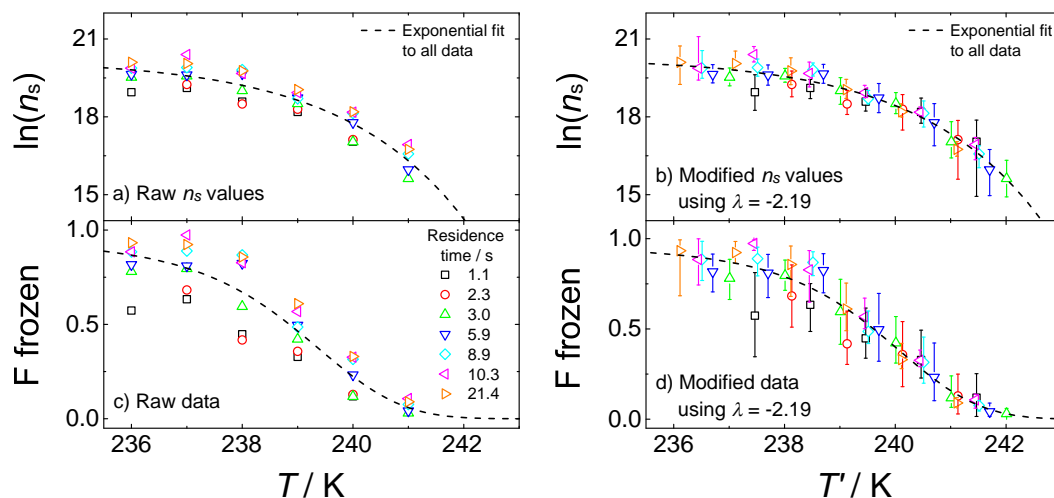


Fig. 8. Raw data for 400 nm kaolinite (K-SA) isothermal experiments from Welti et al. (2012) and normalised data using $\lambda = -2.19$, as determined through minimisation of modified data using $T' = T_{\text{experiment}} + \beta(t)$. **(a)** and **(c)** show the raw n_s values and fraction frozen data respectively, for a series of isothermal experiments. **(b)** and **(d)** show the same datasets where the observed freezing temperature has been modified by $\beta(t)$. Error bars are reproduced from Welti et al. (2012) and for clarity are only shown in the modified datasets. Exponential functions fit to $\ln(n_s)$ resulted in RMSE values of 0.076 and 0.047 for the raw and modified data, respectively. Using these functions, fraction frozen curves were reproduced and are shown as dashed lines in **(c)** and **(d)**.

Title Page

Abstract

Introduction

Conclusions

References

Tables

Figures

◀

▶

◀

▶

Back

Close

Full Screen / Esc

Printer-friendly Version

Interactive Discussion



Representing time-dependent freezing behaviour

R. J. Herbert et al.

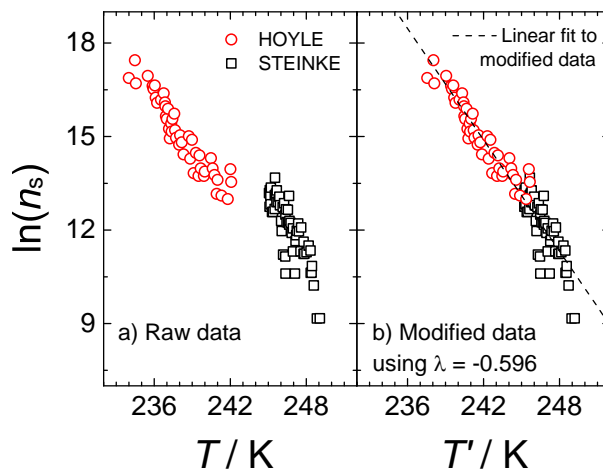


Fig. 9. Nucleation coefficient (n_s) against temperature for a single volcanic ash sample from the Eyjafjallajökull eruption in 2010. Red circles represent data presented in Hoyle et al. (2011) using the ZINC instrument, and black squares represent data from Steinke et al. (2011) using the AIDA expansion chamber. **(a)** Shows the original data, and **(b)** the normalised data. A representative value of λ was determined through the minimisation of modified n_s data using a linear function, resulting in $\lambda = -0.596$. The subsequent fit has a gradient, $d\ln(n_s)/dT$, of -0.596 (equal to λ) which suggests this volcanic ash sample has a uniform nucleating ability and behaves as a single-component system.

Title Page

Abstract

Introduction

Conclusions

References

Tables

Figures

◀

▶

◀

▶

Back

Close

Full Screen / Esc

Printer-friendly Version

Interactive Discussion



Representing time-dependent freezing behaviour

R. J. Herbert et al.

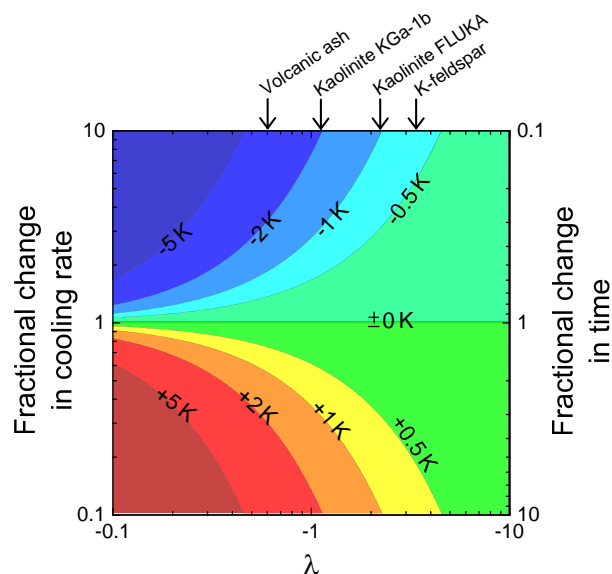


Fig. 10. The shift in temperature β that will result from a fractional change in cooling rate or residence time for a specific value of λ . The values of λ determined for the four IN samples used in this study are also indicated: volcanic ash refers to the HOYLE/STEINKE Eyjafjallajökull ash dataset, Kaolinite KGA-1b to kaolinite, Kaolinite FLUKA to the mineral dust from WELTI, and finally K-feldspar.

Title Page

Abstract

Introduction

Conclusions

References

Tables

Figures

◀

▶

◀

▶

Back

Close

Full Screen / Esc

Printer-friendly Version

Interactive Discussion

